Inhibition of *p*-aminobenzoate and folate syntheses in plants and apicomplexan parasites by the natural product rubreserine*

Djeneb Camara[1]; Cordelia Bisanz[2]; Caroline Barette[3]; Jeroen Van Daele[4]; Esmare Human[5]; Bernice Barnard[5]; Dominique Van Der Straeten[6]; Christophe P. Stove[4]; Willy E. Lambert[4]; Roland Douce[1]; Eric Maréchal[1]; Lyn-Marie Birkholtz[5]; Marie-France Cesbron-Delauw[2]; Renaud Dumas[1] and Fabrice Rébeillé[1]

[1]Laboratoire de Physiologie Cellulaire Végétale, CEA / CNRS UMR5168 / INRA USC1200 / Université Joseph Fourier Grenoble I, Institut de Recherches en Technologies et Sciences pour le Vivant, CEA-Grenoble, F-38054 Grenoble, France
[2]Laboratoire Adaptation et Pathogénie des Microorganismes, CNRS UMR 5163 / Université Joseph Fourier Grenoble I, Institut Jean Roget, F-38042 Grenoble, France

[3]Centre de Criblage pour Molécules Bioactives, Institut de Recherches en Technologies et Sciences pour le Vivant, CEA-Grenoble, F-38054 Grenoble, France
[4]Laboratory of Toxicology, Ghent University, Harelbekestraat 72, B-9000 Ghent, Belgium
[5]Malaria Research Group, Department of Biochemistry, University of Pretoria, Private Bag x20, Pretoria, South Africa, 0028
[6] Laboratory of Functional Plant Biology, Department of Physiology, Ghent University, K.L. Ledeganckstraat 35, B-9000 Ghent, Belgium

*Running title: *Inhibition of pABA synthesis in plants and apicomplexans*.

To whom correspondence should be addressed: Fabrice Rébeillé: PCV/iRTSV, CEA-Grenoble, 17 avenue des Martyrs, F-38054 Grenoble, France ; email : frebeille@cea.fr; Tel: 33 (0)4 38 78 44 93; Fax: 33 (0)4 38 78 50 91

Key words: pABA biosynthesis; GAT-ADCS; folate; Arabidopsis; Apicomplexa;

Background: pABA biosynthesis is a potential target for antifolate drugs.
Results: Rubreserine inhibits GAT-ADCS, an enzyme involved in pABA biosynthesis, and decreased the folate content in *Arabidopsis* and *Toxoplasma.*
Conclusion: Specific inhibition of pABA synthesis induces growth limitation of plants and apicomplexan parasites.
Significance: GAT-ADCS is a valuable target in eukaryotes, and rubreserine is a novel scaffold for anti-parasitic drugs.

SUMMARY

Glutamine amidotransferase / aminodeoxychorismate synthase (GAT-ADCS) is a bifunctional enzyme involved in the synthesis of *p*-aminobenzoate (pABA), a central component part of folate cofactors. GAT-ADCS is found in eukaryotic organisms autonomous for folate biosynthesis, such as plants or parasites of the phylum Apicomplexa. Based on an automated screening to search for new inhibitors of folate biosynthesis, we found that rubreserine was able to inhibit the GAT activity of the plant GAT-ADCS with an apparent IC_{50} of about 8 µM. The growth rates of *Arabidopsis thaliana, Toxoplasma gondii* and *Plasmodium falciparum* were inhibited by rubreserine with respective IC_{50} values of 65, 20 and 1 µM. The correlation between folate biosynthesis and growth inhibition was studied with *Arabidopsis* and *Toxoplasma.* In both organisms the folate content was decreased by 40 - 50 % in the presence of rubreserine. In both organisms, the addition of pABA or 5-formyltetrahydrofolate in the external medium restored the growth for inhibitor concentrations up to the IC_{50} value, indicating that, within this range of concentrations, rubreserine was specific for folate biosynthesis. Rubreserine appeared to be more efficient than sulfonamides, antifolate drugs known to inhibit the invasion and proliferation of *Toxoplasma gondii* in human fibroblasts. Altogether, these results validate the use of the bifunctional GAT-ADCS as an

efficient drug target in eukaryotic cells, and indicate that the chemical structure of rubreserine presents interesting anti-parasitic (toxoplasmosis, malaria) potential.

Folates are a family of cofactors that are essential for cellular one-carbon (C1) transfer reactions. They are involved in several important metabolic pathways, such as the synthesis of nucleotides and the methylation cycle (1-3). Folate biosynthesis can be divided into three branches (Fig. 1A): the first one for the pterin ring synthesis, the second one for the pABA synthesis and the third one for the assembly of these two precursors plus glutamates to form the backbone of folate derivatives (4-6). Blocking folate biosynthesis or turnover leads to the arrest of cell division and eventually to cell death. Antifolate drugs have been developed to exploit this feature in therapies against cancer cells and microbial or parasitic infections. Biosynthesis of folate is mainly inhibited by two groups of compounds, i.e. inhibitors of dihydropteroate synthase (DHPS) and inhibitors of dihydrofolate reductase (DHFR). Inhibitors of DHFR are commonly used as therapeutic agents against cancer (7) whereas a combination of these two types of inhibitors are commonly used in clinical treatments against parasites of the Apicomplexa phylum, such as *Plasmodium falciparum* or *Toxoplasma gondii* (8,9). However, the use of these drugs is compromised by the emergence of resistance, and the currently used chemical scaffolds and protein targets are actually over-exploited. Nevertheless, the long-established efficacy of folate metabolism as a clinical target is strongly encouraging to identify new inhibitors acting against other enzymes of the folate pathway comprising nine enzyme activities in addition to DHPS and DHFR (Fig. 1A) (10-12).

Among potential targets, the enzymes involved in the pABA branch of the pathway are of great interest (13). Indeed, they are absent in animals and the only known metabolic fate of pABA is its commitment in folate synthesis. In addition, it was recently shown in plants that the production of pABA, together with the production of pterins, is rate limiting for the whole folate pathway (4,5). Also, it was shown in *P. falciparum* that pABA was an effective salvage substrate in experiments using antifolates, suggesting that pABA metabolism might offer opportunities for chemotherapy (14). The pABA moiety is synthesized in two steps from chorismate [a metabolite also involved in aromatic amino acid synthesis (15)]. First, chorismate is aminated to form 4-amino-4-deoxychorismate (ADC), and then ADC is aromatized with loss of pyruvate (Fig. 1B). In many bacteria such as *E. coli* or *B. subtilis*, ADC synthesis requires two separate proteins: PabA (a glutamine amidotransferase) and PabB (the ADC synthase) (16). In eukaryotes, the situation appears different. Indeed, in plants and lower eukayotes, such as yeast and Apicomplexa, ADC synthesis is catalyzed by a single bifunctional protein (Fig. 1A) containing two domains, the glutamine amidotransferase (GAT) in the N-terminal part and the ADC synthase (ADCS) in the C-terminus (17). Based on sequence similarities with TrpG (the component II of anthranilate synthase), GAT-ADCS is classified as a member of the G-type group of amidotransferases (18,19). There is only one gene coding for GAT-ADCS in apicomplexan parasites and plants, and a mutation in the plant gene is embryo defective. The ADCS domain belongs to the group of chorismate-utilizing enzymes, which also contains salicylate synthase, isochorismate synthase and anthranilate synthase (20,21). Until now, searches of inhibitors for this class of enzymes were only achieved using prokaryotic systems. They involved docking studies and design of chorismate analogous compounds (22-25), combinatorial chemistry approaches (26,27), and a specific screening of a microorganism extract collection using growth inhibition of test bacteria as a marker of activity (28,29). Several compounds were identified by these different methods but appeared to be relatively weak inhibitors of ADCS, although some of them could be quite potent against other chorismate-utilizing enzymes (22-24,26). The most potent inhibitor of ADCS reported to date is an analogue of chorismate (2-hydroxy-4-amino-4-deoxychorismate), exhibiting a K_i value of 38 µM against the purified enzyme (23). To our knowledge, the *in vivo* effects of these ADCS inhibitors have not been investigated.

In the present report, using a purified recombinant plant GAT-ADCS as a model enzyme for bifunctional GAT-ADCS, we screened a chemical library for new inhibitors of pABA synthesis. We identified one compound exhibiting a K_i < 10 µM and measured the impact of this molecule on a plant (*Arabidopsis thaliana*) and two apicomplexan parasites (*T. gondii* and *P. falciparum*).

EXPERIMENTAL PROCEDURES

Materials - *Arabidopsis thaliana* (ecotype Columbia) seedlings were grown on plates containing Murashige and Skoog medium, 15% agar, plus the various molecules to be tested. Seeds were first sterilized by soaking for 15 min in a solution containing 0.095% Tween and 0,57 % sodium hypochlorite before to be laid on the agar medium. The plates were conserved in the dark at 4 °C for 48 hours then transferred in a green house (20 °C, 80% humidity, 150 $\mu E.m^{-2}.s^{-1}$, 12 h light period). The number of seedlings at the two leaf stage (rosette stage) was counted after 2 weeks.

Arabidopsis thaliana (ecotype Columbia) cell suspension cultures were grown and sub cultured as previously described (30). For measurements of metabolites, cells were collected after 7 days of treatment, rapidly washed with distilled water, weighted, frozen in liquid nitrogen and stored at -80 °C for later analyses.

Toxoplasma gondii tachyzoites from the RH-YFP_2 strain (kindly provided by B. Striepen, Athens, USA) were propagated in human foreskin fibroblasts (HFF) under standard procedures as previously described (31). Invasion and proliferation assays were performed onto HFF cells grown to confluence on glass coverslips in 4 or 24 multiwell plates. For the invasion assay, freshly egressed RH-YFP_2 parasites were incubated for 5 hours with or without the different drugs. To perform synchronized invasion, 10^6 parasites / well were centrifuged for 30 sec at 1300 rpm onto HFF monolayers, and wells were incubated for 15 min in a water bath at 37 °C. Wells were further washed three times with cold PBS to eliminate extracellular parasites. Infected cells were fixed in 5% formaldehyde / PBS for 30 min and stored in PBS at 4 °C until staining. To distinguish intracellular from remaining extracellular parasites, coverslips were incubated with the primary antibody mAb Tg05-54 against the major Toxoplasma surface protein SAG1 (TgSAG1), and then with Texas Red-conjugated goat anti-mouse secondary antibody (Molecular Probes). Intracellular parasites exhibiting a faint red colour can easily be distinguished from extracellular parasites which are in bright red. Nuclei were stained with Hoechst 33258 (Molecular Probes). The number of intracellular parasites was determined from 12 randomly selected fields per coverslip and per experiment with a Zeiss Axioplan 2 microscope equipped for epifluorescence and phase-contrast. Invasion was expressed as % of the number of intracellular parasites recorded in non-treated cells.

To assess the effect of the drugs on intracellular growth of *T. gondii* (proliferation assay), HFF monolayers were infected with 10^5 parasites / well (cf invasion assay). Wells were then washed three times with PBS to eliminate extracellular parasites and drugs were added. After 24 hours at 37 °C in a humidified atmosphere containing 5% CO_2, cells were fixed and stained with Hoechst 33258 as described above. For each drug concentration, the number of parasites was determined from at least 100 individual vacuoles.

To determine folate concentrations, parasites were grown for 24 h in HFF cells in the presence or absence of 20 or 40 µM rubreserine. Then infected HFF monolayers were washed three times with PBS, harvested with a cell scraper and passed four times through a 27-gauge needle to break the cells. Broken cells and released parasites were washed three times with PBS and then parasites were purified by filtration through a 3 µm Nucleopore membrane, further washed two times in PBS, concentrated by centrifugation and frozen at -80 °C until use.

Plasmodium falciparum (3D7) was maintained in human O^+ erythrocytes as previously described (32). The *in vitro* anti-plasmodial activity of the rubreserine was determined using the malaria SYBR Green I fluorescence assay as described (33,34). *In vitro* ring-stage intra-erythrocytic *P. falciparum* parasites (1% haematocrit, 1% parasitaemia) were incubated with specific concentrations of rubreserine in complete *P. falciparum* culture medium, with chloroquine disulphate used as a positive control (0.5 µM) or vehicle (1xPBS) as negative control. Fluorescence was measured after 96 h under drug pressure (excitation 485 nm, emission 538 nm). The data, after subtraction of background (chloroquine disulphate treated iRBCs, no parasite growth) were expressed as percentage of untreated control to determine cell proliferation.

Rubreserine preparation - Rubreserine was prepared from (-)-eseroline fumarate salt (Sigma). Stock solutions of eseroline (10 mM) were made in 50 mM Pi (pH 8), 50 mM Tris (pH 8) or 1 x PBS (pH 7.5) buffers, depending on the experiment. Under these conditions, eseroline is spontaneously oxidized into rubreserine, a process completed in about 6 hours at room temperature. The formation of rubreserine was controlled through the appearance of a characteristic peak of absorption at 475 nm. These stock solutions were stored at 4 °C for 48

h or at -20 °C for one week. They were serially diluted before use.

Expression and purification of the recombinant Arabidopsis enzymes - *At*GAT-ADCS and *Ec*ADCL proteins were expressed and purified as previously described (19). *Arabidopsis* cDNAs encoding GMPS, β-subunit of AS starting at A51 to remove the plastid transit peptide, and α-subunit of AS starting at A61 were amplified by PCR and cloned into the expression vector pET28 (Novagen). *E. coli* BL21-CodonPlus (DE3)-RIL cells (Stratagene) were transformed and grown using the same protocol than for *At*GAT-ADCS. Cells were disrupted and His-tagged recombinant proteins were purified as described (19).

Determination of enzyme activities - GAT activity can be determined by measuring the production of glutamate, and ADCS activity by the production of pABA (19). Standard assays contained 100 mM Tris/HCl (pH 8.0), 5 mM $MgCl_2$, 5% V/V glycerol, 0 to 0.5 mM L-glutamine, 0 to 0.02 mM chorismate, and 9 µg ml^{-1} of the recombinant plant enzyme. The presence of an excess of *Ec*ADCL (20 µg ml^{-1}, 600 nM) is required for the production of pABA. Reactions (final volume 80 µl) were run in 96 well microplates (Greiner) and changes in fluorescence were continuously monitored with a microplate scanning spectrophotometer Safir^2 (Tecan). To monitor glutamate production, an excess of GDH (100 µg ml^{-1}, 4.2 units ml^{-1}) and 1 mM NAD were added to the assay, and NADH production was followed by its emission at 450 nm (excitation 340 nm). Concentration of pABA was monitored by its fluorescence emission at 340 nm (excitation 290 nm) in the presence of *Ec*ADCL.

The activities of GMPS and AS (β- plus α-subunits) were measured monitoring glutamate production. In both conditions the final volume was 500 µl. For GMPS, the assay medium contained: 200 µM XMP, 1 mM ATP, 0.5 mM L-glutamine, 10 µg GMPS, 1 mM NAD, 4.2 units ml^{-1} GDH. For AS, the assay medium contained: 50 µM chorismate, 0.5 mM L-glutamine, 10 µg TrpG, 10 µg TrpE, 1 mM NAD, 4.2 units ml^{-1} GDH and various concentrations of rubreserine. The reactions were started by addition of glutamine and the change in absorbance at 340 nm was monitored with a UV-visible spectrophotometer (Safas).

High throughput screening - The screening was conducted at the Center for the screening of Bio-Active Molecules (CMBA) located at the CEA-Grenoble, France. The library of compounds was purchased from The Prestwick Chemical Library® (http://www.prestwickchemical.com). This library contains 1200 molecules selected for their high chemical and pharmacological diversity. They are marketed and 100% FDA approved compounds, supplied in the library at a 10 mM concentration in DMSO. The final concentration used in the enzymatic assay was 100 µM, and we verified in separate control experiments that 2% DMSO had no effect on the activity. The enzymatic test used for primary and secondary screenings was identical to the one described above for the GAT activity. Quality of the assay was assessed based on the calculation of the Z' factor, as defined by Zhang et al. (35). After optimization of the assay, the Z' factor was 0.76 ± 0.08 (a good assay must display a Z' factor > 0.5). The assay was conducted as follows: 50 µl of a mix containing 0.1 M Tris (pH 8), 5 mM $MgCl_2$, 5% glycerol, 40 µM chorismate, 1 mM NAD, 0.4 unit GDH, 0.7 µg GAT-ADCS and 100 µM of the various molecules were added in each well (in control wells, molecules were omitted). The reaction was started by injection in each well of 30 µl of a solution containing 1.3 mM Gln, and the fluorescence changes (Exc 340 nm, Emi 450 nm) were recorded at 0, 15 and 25 min. The most promising molecules were purchased and their inhibitory properties were manually confirmed.

Measurements of metabolites - Determinations of folates and pABA were essentially performed as described (36-38). Briefly, the extract corresponding to 3 - 5 x 10^7 parasites or 0.5 g (fresh weight) of plant material was subjected to separation using UPLC (for folates) or HPLC (for pABA), followed by tandem mass spectrometric detection on an Applied Biosystems API 4000 (Foster City, CA, USA), using electrospray ionization, in the MRM mode. For folates, the final quantitative data reflect the sum of six different folate monoglutamates: tetrahydrofolate (THF), 5-methyl-THF, 10-formyl-folic acid, 5,10-methenyl-THF, folic acid, and 5-formyl-THF (5-FTHF). [^{13}C]-folate derivatives and 3-NH_2-4-CH_3-benzoic acid were added in the extraction buffers as internal standards for folates and pABA, respectively.

RESULTS

GAT-ADCS assay, high throughput screening and GAT-ADCS inhibition - The

search for enzyme inhibitors by global approaches requires methods to determine the activity that are accurate, robust and compatible with the automated platforms used for screening of chemical libraries. When coupled with glutamate dehydrogenase (GDH), GAT activity was easily measurable with a UV-visible spectrophotometer (340 nm) or a fluorimeter (excitation 340 nm, emission 450 nm) monitoring NADH accumulation (19,39). Also, it was convenient to use the same procedure to test the inhibitors on GDH alone, in order to discard molecules that were specific for this last activity. Based on this protocol, we designed a miniature assay easily reproducible and optimized for the identification of active drugs, with a screening coefficient Z' [a statistical parameter measuring the quality of the screening assay (35)] of 0.76 ± 0.08 (see Experimental procedures). Because all our attempts to produce active recombinant GAT-ADCS from apicomplexan parasites failed, we used the recombinant plant enzyme as a model for this bifunctional system. We screened the registered Prestwick® Chemical Library (1200 compounds) against the GAT activity of the plant GAT-ADCS. After primary and secondary screenings, we identified only four molecules exhibiting IC_{50} values that were below 50 µM. They were manually tested and we found that rubreserine [1,3a,8-trimethyl-1,2,3,3a,8,8a-hexahydropyrrolo[2,3-b]indole-5,6-dione, an oxidative product of eseroline (40-42) that spontaneously forms at alkaline pH (Fig. 2 and Fig. S1 in Supplemental Data)] exhibited the best inhibitory properties. Eseroline itself had no effect, indicating that the carbonyl functions resulting from eseroline oxidation were essential for the inhibition. The rate constant of inhibition was rather low (about 0.1 min^{-1}) and a 20 min period of incubation with rubreserine was required to obtain maximal inhibition. We observed GAT-ADCS inhibition independently of the presence or position of the His-tag that was added for purification convenience, indicating that such a tag was not involved in the inhibition process. We previously showed that the GAT activity was maximal in the presence of chorismate as substrate of the ADCS domain, but could also operate independently (19). We observed inhibition of glutamate production in both conditions, i.e. with and without chorismate, and we also observed inhibition of pABA synthesis when GAT-ADCS was coupled with non limiting amounts of ADC lyase (Fig. 3A, 3B). In separate control experiments we verified that rubreserine did not impact ADC lyase activity. In all situations, rubreserine decreased the V_m and increased the K_m for glutamine, indicating a mixed-type inhibition (Fig. 3C). Apparent equilibrium constants K_i (representing the ratio [E][I]/[EI]) and αK_i, (representing the ratio [ES][I]/[ESI]) calculated from such pattern of curves (43) were estimated to be respectively 3 ± 1 and 8 ± 1 µM in the different conditions, i.e. measuring either glutamate or pABA productions.

In vivo effects of rubreserine on Arabidopsis thaliana growth and folate content - When *Arabidopsis* seedlings were grown on agar plates in the presence of rubreserine concentrations ranging from 50 to 100 µM, we observed a dose-dependent growth inhibition (Fig. 4). Interestingly, when the agar plates were supplemented with pABA, the growth was restored for inhibitor concentrations up to 50 µM, and partially restored for higher concentrations, the maximal effect being obtained with pABA concentrations ≥ 100 µM (Fig. 4). This suggests that for low rubreserine concentrations, at least, the growth inhibition was due to a limitation of pABA synthesis. Because pABA is required for folate biosynthesis, we also measured the potential impact of 5-formyl-THF (5-FTHF) on rubreserine-treated plants (Fig. 4). As shown, this folate derivative had similar effect than pABA.

Next, we investigated the effect of rubreserine on the folate content. We used Arabidopsis cell cultures for these experiments to dispose of enough material for metabolite determinations. For rubreserine concentrations within the range 25 - 100 µM, the cell division came to an arrest after about seven days. Similar results were obtained in the presence of sulfanilamide, a well-known specific inhibitor of DHPS that blocks pABA utilization in the folate pathway (Fig. 1A). After seven days, the pools of folate in rubreserine- and sulfanilamide-treated cells (Table I) decreased by about 40 and 60%, respectively. However, the distributions of folate derivatives were not markedly modified [in all situations, the various representative pools of folates were roughly: 50% 5-methyl-THF, 35% 10-formyl-THF plus 5,10-methenyl-THF, 8% 5-FTHF, 7% THF plus 5,10-methylene-THF, and 0.3% folic acid (30)]. Interestingly, when 100 µM pABA were present in the culture medium, the folate content in both control and rubreserine-treated cells were almost identical

(Table I), which was clearly indicative of a protective effect of pABA. Since rubreserine inhibited the pABA branch of the folate pathway, we also attempted to measure the pABA content of *Arabidopsis* cells. In plants, pABA was found either as free acid or as a glucose ester conjugate. This last form (> 80% of total pABA) is sequestered in vacuoles and does not directly contribute to folate synthesis (44,45). This makes the determination of free pABA quite difficult because, as previously shown (44), breakdown of the esterified form of folate during sample workup is very difficult to avoid and contributes, sometimes quite significantly, to the amount of free pABA. However, in the presence of 100 µM rubreserine, we observed a small but significant decrease of free pABA by about 30% (Table II). In contrast, the total amount of pABA did not markedly change, suggesting that the glucose ester conjugate in the vacuole and the free acid form in the cytosol are not in rapid equilibrium. In sulfanilamide-treated cells, free and total pABA slightly increased by about 30% (Table II), an expected result taking into account that pABA utilization was blocked (46).

Effect of rubreserine on the proliferation of apicomplexan parasites - Before testing the effect of rubreserine on *Toxoplasma gondii*, we first verified with the MTT [3-(4,5-Dimethylthiazol-2-yl)-2,5-diphenyltetrazolium bromide] cytotoxicity assay (47) that rubreserine concentrations up to 50 µM had no toxicity on confluent human fibroblast (HFF) cells. Indeed, after 48 h of exposure to 50 µM rubreserine, the cell viability was still 95 ± 5% of the control. Then, we evaluated the effect of rubreserine on *Toxoplasma* parasites in two different situations: invasion of confluent HFF by the parasites in one hand, and intracellular development of the parasites within confluent HFF in the other hand. As shown in Figure 5A, invasion of human cells strongly decreased when the parasites had been previously incubated with rubreserine. This effect was dose-dependent, the number of intracellular parasites being reduced two fold in the presence of 20 µM rubreserine (IC_{50}). Likewise, when infected cells were placed in the presence of the inhibitor, the number of parasites in parasitophorous vacuoles decreased after 24 h in comparison with untreated infected cells, which was indicative of a slowing down of the parasite's intracellular division (Fig. 5B). In both situations, rubreserine appeared much more efficient than sulfanilamide and sulfadiazine, this last sulfonamide drug being widely used in the treatment of toxoplasmosis. To correlate the inhibitory effect with folate biosynthesis, we attempted to determine the folate concentration in *T. gondii* cells. To our knowledge, there was no report about the intracellular concentration of folates within proliferating *T. gondii* parasites. We measured folates in parasites grown for 24 h in HFF cells placed in the presence of either 20 or 40 µM rubreserine (Table III). Interestingly, in both conditions the total folate concentration decreased by a factor of two. Also, similar to what was observed in plants, the distributions of folate derivatives were not significantly changed in the presence of the drug (in these cells the various representative pools of folates were: 18% 5-methyl-tetrahydrofolate, 25% 10-formyl-tetrahydrofolate plus 5,10-methenyl-tetrahydrofolate, 42% 5-FTHF, 8% tetrahydrofolate plus 5,10-methylene-tetrahydrofolate, and 7% folic acid). In addition, for a rubreserine concentration of 20 µM (IC_{50} value), the parasite growth was largely restored in the presence of either pABA or 5-FTHF (Fig. 6A), the maximal protective effect being obtained for concentrations ≥ 25 µM. Thus, for such inhibitor concentration (20 µM), the inhibitory process largely relied on the inhibition of pABA and folate biosynthesis. However, for rubreserine concentrations higher than 20 µM, pABA and 5-FTHF had only little effect (Fig. 6B), suggesting that high concentrations of the inhibitor had other, non folate-specific, actions. Since antifolate drugs (anti DHPS and anti DHFR) are often used in combination, we tested the effect of rubreserine in combination with an anti DHFR (Fig. 6C). When 20 µM rubreserine and 0.4 µM pyrimethamine were combined, the inhibition was slightly but significantly increased compared to rubreserine alone. Interestingly, rubreserine alone appeared in our experimental conditions as efficient as a mixture combining 50 µM sulfadiazine and 0.4 µM pyrimethamine.

Additionally, rubreserine was also tested on the *in vitro* proliferation of *P. falciparum*. As shown in Figure 7, rubreserine exhibited anti-malarial properties since the intraerythrocytic growth of the parasite was strongly inhibited by rubreserine, with an IC_{50} of 1 ± 0.04 µM (n=5). Whether folate biosynthesis is also a primary target in these organisms is currently under investigation.

Specificity of inhibition by rubreserine - At low rubreserine concentrations, folate biosynthesis appeared as a main target in *Arabidopsis* and *Toxoplasma*. However, at high

rubreserine concentrations the growth activity could not be fully restored by the presence of pABA or 5-FTHF, raising the question of the inhibitor specificity. GAT-ADCS belongs to the family of class I glutamine amidotransferases (18,48), which contains six other members. The GAT domain of GAT-ADCS does not share strong homologies with the GAT domains of the other members of this class, the best scores being obtained with anthranilate synthase (AS, about 28% identity), GMP synthetase (GMPS, about 13% identity) and carbamoyl phosphate synthetase II (involved in UMP synthesis, about 15% identity). To test the effect of rubreserine on other members of this group, we attempted to produce these recombinant *Arabidopsis* activities. We failed to produce active recombinant carbamoyl phosphate synthetase, but we produced AS [a heterodimeric protein combining the activities of β- and α-subunits, respectively equivalent to TrpG and TrpE in prokaryotes (49)] and GMPS [a bifunctional enzyme with fused GAT and synthase domains (50), alike GAT-ADCS]. We determined these activities with the same GDH-coupled assay that we used for GAT-ADCS. As shown in Table IV, rubreserine also inhibited GMPS and AS activities, although inhibition of GMPS required higher concentrations of inhibitor. *Toxoplasma*, but not *Plasmodium,* is auxotroph for tryptophan because of the lack of AS activity (51,52). However, the enzymes involved in the synthesis of GMP [GMPS, a bifunctional enzyme, alike to plants (53)] and UMP [carbamoyl phosphate synthetase II, a heterodimer in plants (54), but a single protein in apicomplexan parasites (55)] are present in these organisms. When a mixture containing pABA, anthranilate, UMP and GMP (100 µM each) was added to the culture medium of rubreserine-treated plants or was present in the proliferation assay of *Toxoplasma*, the growth recovery for both organisms was not markedly improved compared to that obtained with pABA or 5-FTHF alones (see Fig. 6B for the experiments with *T. gondii*).

DISCUSSION

Two main conclusions can be drawn from this study: first, our data validate for the first time the use of the bifunctional GAT-ADCS as an efficient drug target in eukaryotic cells, and, second, we identified a new scaffold that inhibits plant growth and proliferation of apicomplexan parasites.

The screening test we used appeared efficient to select active compounds from Prestwick® chemical library, and we found that an oxidative product of eseroline, rubreserine, was inhibiting the GAT activity of *At*GAT-ADCS. Eseroline and rubreserine were identified a long time ago as metabolites of physostigmine (eserine), an alkaloid present in the Calabar bean (*Physostigma venenosum*), and previously used for its potent anticholinesterase activity. To our knowledge, rubreserine and eseroline have no current use in any medical purpose. Pharmacological studies indicated that these two molecules were not or weak inhibitors of cholinesterase (56), but there was no report indicating that rubreserine could affect folate biosynthesis and inhibit the growth of plants and the proliferation of parasites. Thus, we describe for this compound a new biological effect with interesting therapeutic potentialities.

When GAT-ADCS was coupled with ADC lyase, the apparent constant of inhibition (K_i) for pABA formation was estimated to be < 10 µM, which is the best constant of inhibition obtained so far for the biosynthesis of pABA. How rubreserine affects the protein activity is however not yet understood, and currently under investigation. The obvious difference between the chemical structures of eseroline and rubreserine is the presence of two carbonyl functions on the aromatic ring of the latter compound. Thus, these carbonyl functions were presumably at the origin of the inhibitory effect. It must be noted that many other natural quinonoid compounds were shown to display antimalarial properties (57), although the targets and modes of action were not described for most of them.

The rubreserine-dependent growth inhibitions of *Arabidopsis* and *Toxoplasma* were specifically associated with an inhibition of folate biosynthesis for concentrations ≤ IC_{50}, although higher concentrations might also inhibit other activities. The correlation between rubreserine and folate biosynthesis was observed by direct and indirect approaches. The direct approach indicated that *Arabidopsis* cells exhibited folate and free pABA contents lowered respectively by 45 % and 25 % in the presence of the inhibitor. In addition, when pABA was present in the culture medium of rubreserine-treated plant cells, the folate level was almost identical to the control, indicating a protective role of pABA. Likewise, the folate level in *Toxoplasma* cells was two times lowered by

rubreserine. The impact of rubreserine on folate biosynthesis was also shown indirectly. Indeed, for rubreserine concentrations close to the IC_{50} values, the rubreserine-dependent growth inhibitions of *Arabidopsis* and *Toxoplasma* were for a large part reversed by the addition of pABA or 5-FTHF, indicating that the biosynthesis of pABA displayed a particular sensitivity to rubreserine, and that the resulting decrease of folate biosynthesis contributed to the inhibitory process. The mode of action of rubreserine in *Plasmodium* is currently under investigation to determine to which extent folate biosynthesis is inhibited in this organism, and the contribution of such an inhibition to the whole inhibitory process.

It is interesting to compare the effects of GAT-ADCS and DHPS inhibitors because both types of drugs impact pABA metabolism. Interestingly, rubreserine appeared in our experimental conditions much more efficient against *Toxoplasma gondii* than sulfadiazine, a sulfonamide widely used for the treatment of severe toxoplasmosis. Indeed, the IC_{50} value calculated for rubreserine was significantly lower than the IC_{50} for sulfadiazine estimated from this study (> 50 μM). The IC_{50} for sulfadiazine may fluctuate widely depending on the parasite strain, from about 20 μM to more than 200 μM, and is generally > 30 μM (58). Such a variation presumably illustrates the occurrence of resistance within the numerous *Toxoplasma* strains. Sulfonamide drugs are normally not used alone against parasites of the Apicomplexa phylum because of their limited activity (8). However, they are potent synergizers of DHFR inhibitors (exemplified in Fig. 6B), which is the reason why these molecules are used in combination. Indeed, inhibition of DHPS decreases the *de novo* synthesis of dihydropteroate, which, in turn, leads to reduction of dihydrofolate, the substrate of DHFR. Because the amount of dihydrofolate is decreased, the efficiency of DHFR inhibitors increases and lower doses of these toxic molecules are required. When rubreserine was used in combination with pyrimethamine in *Toxoplasma*, we also observed a small but significant synergistic effect, and such an association appeared as efficient as a mixture combining sulfadiazine and pyrimethamine. Thus, molecules with a hexahydropyrrolo[2,3-*b*]indole-5,6-dione scaffold, such as rubreserine, could be interesting structures to develop novel drugs that could represent alternatives to sulfonamides.

REFERENCES

1. Rébeillé, F., Ravanel, S., Jabrin, S., Douce, R., Storozhenko, S., and Van Der Straeten, D. (2006) Folates in plants: biosynthesis, distribution, and enhancement. *Physiol. Plant.* **126**, 330-342

2. Blancquaert, D., Storozhenko, S., Loizeau, K., De Steur, H., De Brouwer, V., Viaene, J., Ravanel, S., Rebeille, F., Lambert, W., and Van Der Straeten, D. (2010) Folates and Folic Acid: From Fundamental Research Toward Sustainable Health. *Crit. Rev. Plant Sci.* **29**, 14-35

3. Ravanel, S., Douce, R., and Rébeillé, F. (2011) Metabolism of folates in plants. in *Advances in Botanical Research, Vol 59* (Rébeillé, F., and Douce, R. eds.), Elsevier, Amsterdam, The Netherlands. pp 67-106

4. Storozhenko, S., De Brouwer, V., Volckaert, M., Navarrete, O., Blancquaert, D., Zhang, G. F., Lambert, W., and Van Der Straeten, D. (2007) Folate fortification of rice by metabolic engineering. *Nat Biotechnol* **25**, 1277-1279

5. Diaz De La Garza, R., Gregory III, J., and Hanson, A. D. (2007) Folate biofortification of tomato fruit. *Proc Natl Acad Sci U S A* **104**, 4218-4222

6. Rébeillé, F., Alban, C., Bourguignon, J., Ravanel, S., and Douce, R. (2007) The role of plant mitochondria in the biosynthesis of coenzymes. *Photosynth. Res.* **92**, 149-162

7. Bertino, J. R. (2009) Cancer research: from folate antagonism to molecular targets. *Best Practice & Research Clinical Haematology* **22**, 577-582

8. Nzila, A. (2006) Inhibitors of de novo folate enzymes in *Plasmodium falciparum*. *Drug Discov. Today* **11**, 939-944

9. Wang, P., Wang, Q., Aspinall, T. V., Sims, P. F. G., and Hyde, J. E. (2004) Transfection studies to explore essential folate metabolism and antifolate drug synergy in the human malaria parasite Plasmodium falciparum. *Mol. Microbiol.* **51**, 1425-1438

10. Wang, P., Wang, Q., Yang, Y. H., Coward, J. K., Nzila, A., Sims, P. F. G., and Hyde, J. E. (2010) Characterisation of the bifunctional dihydrofolate synthase-folylpolyglutamate synthase from Plasmodium falciparum; a potential novel target for antimalarial antifolate inhibition. *Mol. Biochem. Parasitol.* **172**, 41-51

11. Nzila, A., Ward, S. A., Marsh, K., Sims, P. F., and Hyde, J. E. (2005) Comparative folate metabolism in humans and malaria parasites (part II): activities as yet untargeted or specific to Plasmodium. *Trends Parasitol* **21**, 334-339

12. Rattanachuen, W., Jonsson, M., Swedberg, G., and Sirawaraporn, W. (2009) Probing the roles of non-homologous insertions in the N-terminal domain of Plasmodium falciparum hydroxymethylpterin pyrophosphokinase-dihydropteroate synthase. *Mol. Biochem. Parasitol.* **168**, 135-142

13. Hyde, J. E. (2005) Exploring the folate pathway in Plasmodium falciparum. *Acta Trop.* **94**, 191-206

14. Salcedo-Sora, J. E., Ochong, E., Beveridge, S., Johnson, D., Nzila, A., Biagini, G. A., Stocks, P. A., O'Neill, P. M., Krishna, S., Bray, P. G., and Ward, S. A. (2011) The Molecular Basis of Folate Salvage in Plasmodium falciparum CHARACTERIZATION OF TWO FOLATE TRANSPORTERS. *J. Biol. Chem.* **286**, 44659-44668

15. Siehl, D. (1999) The biosynthesis of tryptophan, tyrosine and phenylalanine from chorismate. in *Plant amino acids* (Singh, B. K. ed.), Marcel Dekker, Inc., New York. pp 171-204

16. Roux, B., and Walsh, C. T. (1992) p-aminobenzoate synthesis in *Escherichia coli*: kinetic and mechanistic characterization of the amidotransferase PabA. *Biochemistry* **31**, 6904-6910

17. Basset, G. J., Quinlivan, E. P., Ravanel, S., Rebeille, F., Nichols, B. P., Shinozaki, K., Seki, M., Adams-Phillips, L. C., Giovannoni, J. J., Gregory, J. F., 3rd, and Hanson, A. D. (2004) Folate synthesis in plants: The p-aminobenzoate branch is initiated by a bifunctional PabA-PabB protein that is targeted to plastids. *Proc Natl Acad Sci U S A* **101**, 1496-1501

18. Zalkin, H. (1993) The amidotransferases. *Adv Enzymol Relat Areas Mol Biol* **66**, 203-309

19. Camara, D., Richefeu-Contesto, C., Gambonnet, B., Dumas, R., and Rébeillé, F. (2011) The synthesis of pABA: Coupling between the glutamine amidotransferase and aminodeoxychorismate synthase domains of the bifunctional aminodeoxychorismate synthase from Arabidopsis thaliana. *Arch. Biochem. Biophys.* **505**, 83-90

20. Ziebart, K. T., and Toney, M. D. (2010) Nucleophile Specificity in Anthranilate Synthase, Aminodeoxychorismate Synthase, Isochorismate Synthase, and Salicylate Synthase. *Biochemistry* **49**, 2851-2859

21. Kerbarh, O., Bulloch, E. M., Payne, R. J., Sahr, T., Rebeille, F., and Abell, C. (2005) Mechanistic and inhibition studies of chorismate-utilizing enzymes. *Biochem Soc Trans* **33**, 763-766

22. Bulloch, E. M., Jones, M. A., Parker, E. J., Osborne, A. P., Stephens, E., Davies, G. M., Coggins, J. R., and Abell, C. (2004) Identification of 4-amino-4-deoxychorismate synthase as the molecular target for the antimicrobial action of (6s)-6-fluoroshikimate. *J Am Chem Soc* **126**, 9912-9913

23. Kozlowski, M. C., Tom, N. J., Seto, C. T., Sefler, A. M., and Bartlett, P. A. (1995) Chorismate-utilizing enzymes isochorismate synthase, anthranilate synthase, and p-aminobenzoate synthase: mechanistic insight through inhibitor design. *J. Am. Chem. Soc.* **117**, 2128-2140

24. Payne, R. J., Bulloch, E. M. M., Toscano, M. M., Jones, M. A., Kerbarh, O., and Abell, C. (2009) Synthesis and evaluation of 2,5-dihydrochorismate analogues as inhibitors of the chorismate-utilising enzymes. *Org Biomol Chem* **7**, 2421-2429

25. Payne, R. J., Bulloch, E. M. M., Kerbarh, O., and Abell, C. (2010) Inhibition of chorismate-utilising enzymes by 2-amino-4-carboxypyridine and 4-carboxypyridone and 5-carboxypyridone analogues. *Org Biomol Chem* **8**, 3534-3542

26. Ziebart, K. T., Dixon, S. M., Avila, B., El-Badri, M. H., Guggenheim, K. G., Kurth, M. J., and Toney, M. D. (2010) Targeting multiple chorismate-utilizing enzymes with a single inhibitor: validation of a three-stage design. *J Med Chem* **53**, 3718-3729

27. Dixon, S., Ziebart, K. T., He, Z., Jeddeloh, M., Yoo, C. L., Wang, X. B., Lehman, A., Lam, K. S., Toney, M. D., and Kurth, M. J. (2006) Aminodeoxychorismate synthase inhibitors from one-bead one-compound combinatorial libraries: "Staged" inhibitor design. *J. Med. Chem.* **49**, 7413-7426

28. Riedlinger, J., Reicke, A., Zahner, H., Krismer, B., Bull, A. T., Maldonado, L. A., Ward, A. C., Goodfellow, M., Bister, B., Bischoff, D., Sussmuth, R. D., and Fiedler, H. P. (2004) Abyssomicins, inhibitors of the para-aminobenzoic acid pathway produced by the marine Verrucosispora strain AB-18-032. *J Antibiot (Tokyo)* **57**, 271-279

29. Keller, S., Schadt, H. S., Ortel, I., and Sussmuth, R. D. (2007) Action of atrop-abyssomicin C as an inhibitor of 4-amino-4-deoxychorismate synthase PabB. *Angewandte Chemie-International Edition* **46**, 8284-8286

30. Loizeau, K., De Brouwer, V., Gambonnet, B., Yu, A., Renou, J. P., Van Der Straeten, D., Lambert, W. E., Rebeille, F., and Ravanel, S. (2008) A Genome-Wide and Metabolic Analysis Determined the Adaptive Response of Arabidopsis Cells to Folate Depletion Induced by Methotrexate. *Plant Physiol.* **148**, 2083-2095

31. Bisanz, C., Bastien, O., Grando, D., Jouhet, J., Marechal, E., and Cesbron-Delauw, M. F. (2006) Toxoplasma gondii acyl-lipid metabolism: de novo synthesis from apicoplast-generated fatty acids versus scavenging of host cell precursors. *Biochem J* **394**, 197-205

32. Allen, R. J., and Kirk, K. (2010) Plasmodium falciparum culture: the benefits of shaking. *Mol Biochem Parasitol* **169**, 63-65

33. Bennett, T. N., Paguio, M., Gligorijevic, B., Seudieu, C., Kosar, A. D., Davidson, E., and Roepe, P. D. (2004) Novel, rapid, and inexpensive cell-based quantification of antimalarial drug efficacy. *Antimicrob. Agents Chemother.* **48**, 1807-1810

34. Smilkstein, M., Sriwilaijaroen, N., Kelly, J. X., Wilairat, P., and Riscoe, M. (2004) Simple and inexpensive fluorescence-based technique for high-throughput antimalarial drug screening. *Antimicrob. Agents Chemother.* **48**, 1803-1806

35. Zhang, J. H., Chung, T. D. Y., and Oldenburg, K. R. (1999) A simple statistical parameter for use in evaluation and validation of high throughput screening assays. *J. Biomol. Screen.* **4**, 67-73

36. Zhang, G. F., Mortier, K. A., Storozhenko, S., Van De Steene, J., Van Der Straeten, D., and Lambert, W. E. (2005) Free and total para-aminobenzoic acid analysis in plants with high-performance liquid chromatography/tandem mass spectrometry. *Rapid Commun Mass Spectrom* **19**, 963-969

37. De Brouwer, V., Zhang, G. F., Storozhenko, S., Van Der Straeten, D., and Lambert, W. E. (2007) pH stability of individual folates during critical sample preparation steps in prevision of the analysis of plant folates. *Phytochem. Anal.* **18**, 496-508

38. De Brouwer, V., Storozhenko, S., Stove, C. P., Van Daele, J., Van Der Straeten, D., and Lambert, W. E. (2010) Ultra-performance liquid chromatography-tandem mass spectrometry (UPLC-MS/MS) for the sensitive determination of folates in rice. *J. Chromatogr. B* **878**, 509-513

39. Sahr, T., Ravanel, S., Basset, G., Nichols, B. P., Hanson, A. D., and Rebeille, F. (2006) Folate synthesis in plants: purification, kinetic properties, and inhibition of aminodeoxychorismate synthase. *Biochem J* **396**, 157-162

40. Poobrasert, O., Chai, H., Pezzuto, J. M., and Cordell, G. A. (1996) Cytotoxic degradation product of physostigmine. *J. Nat. Prod.* **59**, 1087-1089

41. Yang, S. T., Wilken, L. O., and Clark, C. R. (1987) Liquid-chromatographic determination of the ph-dependent degradation of eseroline - hydrolysis product of physostigmine. *J. Pharm. Biomed. Anal.* **5**, 383-393

42. Robinson, B. (1965) Structure of rubreserine a decomposition product of physostigmine. *J. Pharm. Pharmacol.* **17**, 89-91

43. Segel, I. H. (1975) *Enzyme kinetics*, John Wiley and sons, New-York

44. Quinlivan, E. P., Roje, S., Basset, G., Shachar-Hill, Y., Gregory, J. F., 3rd, and Hanson, A. D. (2003) The folate precursor p-aminobenzoate is reversibly converted to its glucose ester in the plant cytosol. *J Biol Chem* **278**, 20731-20737

45. Eudes, A., Bozzo, G. G., Waller, J. C., Naponelli, V., Lim, E. K., Bowles, D. J., Gregory, J. F., and Hanson, A. D. (2008) Metabolism of the folate precursor p-aminobenzoate in plants - Glucose ester formation and vacuolar storage. *J. Biol. Chem.* **283**, 15451-15459

46. Orsomando, G., Bozzo, G. G., de la Garza, R. D., Basset, G. J., Quinlivan, E. P., Naponelli, V., Rebeille, F., Ravanel, S., Gregory, J. F., 3rd, and Hanson, A. D. (2006) Evidence for folate-salvage reactions in plants. *Plant J* **46**, 426-435

47. Mosmann, T. (1983) Rapid colorimetric assay for cellular growth and survival - application to proliferation and cyto-toxicity assays. *J. Immunol. Methods* **65**, 55-63

48. Massiere, F., and Badet-Denisot, M. A. (1998) The mechanism of glutamine-dependent amidotransferases. *Cell. Mol. Life Sci.* **54**, 205-222

49. Zhang, X. H., Brotherton, J. E., Widholm, J. M., and Portis, A. R. (2001) Targeting a nuclear anthranilate synthase alpha-subunit gene to the tobacco plastid genome results in enhanced tryptophan biosynthesis. Return of a gene to its pre-endosymbiotic origin. *Plant Physiol.* **127**, 131-141

50. Nakamura, J., Straub, K., Wu, J., and Lou, L. (1995) The glutamine hydrolysis function of human gmp synthetase - Identification of an essential active-site cysteine. *J. Biol. Chem.* **270**, 23450-23455

51. Sibley, L. D., Messina, M., and Niesman, I. R. (1994) Stable dna transformation in the obligate intracellular parasite *Toxoplasma gondii* by complementation of tryptophan auxotrophy. *Proc Natl Acad Sci U S A* **91**, 5508-5512

52. Roberts, C. W., Roberts, F., Lyons, R. E., Kirisits, M. J., Mui, E. J., Finnerty, J., Johnson, J. J., Ferguson, D. J. P., Coggins, J. R., Krell, T., Coombs, G. H., Milhous, W. K., Kyle, D. E., Tzipori, S., Barnwell, J., Dame, J. B., Carlton, J., and McLeod, R. (2002) The shikimate pathway and its branches in apicomplexan parasites. *J. Infect. Dis.* **185**, S25-S36

53. Bhat, J. Y., Shastri, B. G., and Balaram, H. (2008) Kinetic and biochemical characterization of *Plasmodium falciparum* GMP synthetase. *Biochem. J.* **409**, 263-273

54. Schroder, M., Giermann, N., and Zrenner, R. (2005) Functional analysis of the pyrimidine de novo synthesis pathway in solanaceous species. *Plant Physiol.* **138**, 1926-1938

55. Fox, B. A., and Bzik, D. J. (2002) De novo pyrimidine biosynthesis is required for virulence of Toxoplasma gondii. *Nature* **415**, 926-929

56. Ellis, S., Krayer, O., and Plachte, F. L. (1943) Studies on physostigmine and related substances. III. Breackdown products of physostigmine; their inhibitory effect on cholinesterase and theit pharmacological action. *Pharmacol. Exp. Ther.* **79**, 309-319

57. Kaur, K., Jain, M., Kaur, T., and Jain, R. (2009) Antimalarials from nature. *Bioorganic & Medicinal Chemistry* **17**, 3229-3256

58. Meneceur, P., Bouldouyre, M. A., Aubert, D., Villena, I., Menotti, J., Sauvage, V., Garin, J. F., and Derouin, F. (2008) In vitro susceptibility of various genotypic strains of Toxoplasma gondii to pyrimethamine, sulfadiazine, and atovaquone. *Antimicrob. Agents Chemother.* **52**, 1269-1277

Acknowledgments - We wish to thank Bernadette Gambonnet for technical assistance, Dr Céline Richefeu-Contesto for helpful discussions and Drs Stéphane Ravanel and Claude Alban for critical reading of the manuscript.

FOOTNOTES

*This work and the Ph.D. fellowship of D.C. were supported by the Région Rhône-Alpes (Cluster 9, 'Plantacter'). E.M. was supported by an ANR PlasmoExpress grant. D.V.D.S. and W.L. thank Ghent University for financial support (BOF09-GOA-004).
A patent was registered in the European Patent Office: patent number 11290215.0 – 1211.
The abbreviations used are: pABA, *para*-aminobenzoic acid; GAT-ADCS, glutamine amidotransferase - aminodeoxychorismate synthase; ADCL, aminodeoxychorismate lyase; AS, anthranilate synthase; GMPS, GMP synthetase; GDH, glutamate dehydrogenase; THF or H_4FGlu_n, tetrahydrofolate; 5-FTHF, 5-formyl tetrahydrofolate; Rubre, rubreserine; Sulfa, sulfanilamide; SDZ, sulfadiazine.

FIGURE LEGENDS

FIGURE 1. Biosynthesis of THF. A) Schematic representation of the pathways found in *E. coli, P. falciparum* and *A. thaliana*. The enzymes involved are: 1, GTP cyclohydrolase I; 2, NUDIXhydrolase; 3, unspecific phosphatase; 4, dihydroneopterin aldolase; 4', 6-pyruvoyltetrahydropterin synthase; 5, glutamine amidotransferase (GAT) and aminodeoxychorismate synthase (ADCS) (PabA and PabB in *E. coli*); 6, ADC lyase (ADCL); 7, 6-hydroxymethyldihydropterin (H_2Pterin) pyrophosphokinase; 8, dihydropteroate (H_2Pteroate) synthase; 9, dihydrofolate (H_2F) synthetase; 10, dihydrofolate reductase; 11, folylpolyglutamate synthetase; 12, thymidylate synthase. Other abbreviations: Cho, chorismate; pABA, *p*-aminobenzoate; H_2PterinPP, 6-hydroxymethyldihydropterin pyrophosphate; H_4F, tetrahydrofolate; H_4F-Glu_n, the polyglutamylated form of H_4F. Merged symbols represent bifunctional enzymes. The activities 9 and 11 are catalyzed by a single enzyme in *E. coli* and *Plasmodium*. In *Plasmodium*, the activity 6 remains to be identified. Above the broken line, the activities are absent in animals. The black stars show the two enzymes actually targeted by antifolate drugs. The white stars show the potential target studied in the present paper. B) Details of the two-step pathway required for pABA synthesis. In all eukaryotes the first step involves a bifunctional GAT-ADCS, whereas two separate proteins PabA and PabB are found in most (but not all) prokaryotes (19).

FIGURE 2. Chemical structures of eseroline and rubreserine. Oxidation of eseroline into rubreserine is spontaneous and strongly increased at pH > 7.

FIGURE 3. Effect of rubreserine on GAT-ADCS kinetics. A) Glutamine-dependent glutamate production (GAT activity alone, no chorismate) in the presence of rubreserine. GAT-ADCS was first incubated with the various concentrations of rubreserine for 20 min, and then the kinetic was started by the addition of Gln, NAD and GDH. B) Glutamine-dependent pABA production (GAT-ADCS activity, 100 µM chorismate) in the presence of rubreserine and non-limiting amount of ADCL. GAT-ADCS was first incubated with the various concentrations of rubreserine for 20 min, and then the kinetic was started by the addition of Gln, chorismate and ADCL. C) Reverse plot of Figure 3B. Maximal rates of the recombinant enzyme were 140 ± 40 nmol min^{-1} mg^{-1} for GAT activity (glutamate

production, no chorismate) and 130 ± 30 nmol min^{-1} mg^{-1} for GAT-ADCS activity (pABA production, with chorismate and ADCL). Curves were fitted with the hyperbolic equation of Michaelis-Menten (3A and 3B) and linear regression (3C). All our assays were made in triplicate and expressed ± SD.

FIGURE 4. Effect of rubreserine on the development of *Arabidopsis* seedlings. Seedlings were grown in agar plates without (controls) or with 50, 75 or 100 µM rubreserine. The estimated number of seedlings at the rosette stage after 2 weeks is expressed as % of the conditions without rubreserine. The presence in the culture medium of 200 µM pABA or 200 µM 5-FTHF partially reversed the growth inhibition. Results are the average of at least three independent experiments ± SD. Asterisks mark datasets showing statistical difference with the condition containing rubreserine alone in a Student's T-test ($p < 0.05$).

FIGURE 5. Effect of rubreserine (Rubre) on invasion and proliferation of *T. gondii*, and comparison with sulfanilamide (Sulfa) and sulfadiazine (SDZ). A) Invasion of human fibroblasts. The parasites were first incubated with the various drugs for 5 h, and then placed in contact with HFF cells for 15 min. The number of intracellular parasites is expressed for each experiment as % of the number recorded in non-treated cells. B) Intracellular growth of the parasites. Proliferation was estimated 24 h after the invasion process and expressed as the number of parasites present in the parasitophorous vacuoles. Results from invasion and proliferation experiments are the average of three to four independent experiments ± SD.

FIGURE 6. Effect of rubreserine in combination with various other compounds on the proliferation of *T. gondii*. The number of parasites present in the parasitophorous vacuoles after 24 h are expressed as % *versus* the corresponding controls (i.e. no adds, or pABA alone, or 5-FTHF alone). A) Reverse effect of pABA and 5-FTHF in the presence of 20 µM rubreserine (Rubre). B) Reverse effect of pABA and 5-FTHF (100 µM each) as a function of rubreserine concentration. C) Effect of various drug combinations; the concentrations used were: 20 µM rubreserine (Rubre), 0.4 µM pyrimethamine (Pyrim), 100 µM pABA, 100 µM 5-formyltetrahydrofolate (5-FTHF), 50 µM sulfadiazine (SDZ). Mix is a mixture containing pABA, anthranilate, UMP and GMP, 50 µM each. Asterisks indicate statistical difference in a Student's T-test ($p < 0.05$) between the conditions rubreserine alone and rubreserine in combination with other drugs, and between the conditions sulfadiazine or pyrimethamine alone and sulfadiazine plus pyrimethamine. Results are the averages of 3 to 4 independent experiments ± SD.

FIGURE 7. Effect of rubreserine on the growth of *P. falciparum*. Parasites were maintained under normal culture conditions and exposed to serial dilutions of rubreserine from 10 mM and parasite proliferation determined as a measurement of DNA content with SYBR Green I fluorescence after 96 h of exposure. Data are averaged from 5 independent experiments performed in triplicate (± SD).

Table I. Effect of rubreserine (Rubre) on the folate content of *Arabidopsis* cells, and comparison with sulfanilamide (Sulfa). Cells were cultivated for 7 days with the various compounds before folate determinations. The total folate contents of control cells cultivated with or without 100 µM pABA were respectively 11.8 ± 2 and 10 ± 1.5 nmoles g^{-1} fresh weight. Measurements are the average ± SD of 4 to 6 determinations from 2 to 3 independent set of experiments. Results for each set of experiment are expressed as % versus the corresponding control.

Conditions	Total folates (% *versus* control)
Rubre 25 µM	60 ± 10
Rubre 25 µM + pABA 100 µM	85 ± 9
Rubre 50 µM	66 ± 3
Rubre 50 µM + pABA 100 µM	116 ± 12
Rubre 100 µM	54 ± 9
Sulfa 25 µM	42 ± 3
Sulfa 100 µM	39 ± 6

Table II. Effect of rubreserine (Rubre) on the pABA contents of *Arabidopsis* cells, and comparison with sulfanilamide (Sulfa). Cells were cultivated for 7 days with the various compounds before pABA determination. The total and free pABA concentrations found in control cells were respectively 8.5 ± 2 and 1.1 ± 0.4 nmoles g^{-1} fresh weight. Measurements are the average ± SD of 8 determinations from 4 sets of experiments. Results for each set of experiments are expressed as % versus the corresponding control.

Conditions	pABA (% *versus* control)	
	Total	Free
Rubre 100 µM	90 ± 5	73 ± 8
Sulfa 100 µM	128 ± 16	132 ± 18

Table III. Effect of rubreserine (Rubre) on the folate content of *Toxoplasma gondii* cells. Parasites were grown for 24 hours in confluent HFF cells in the presence of 20 or 40 μM rubreserine. The results are expressed as nmoles per 10^7 parasites. Measurements are the average ± SD of 2 (40 μM Rubre), 3 (20 μM Rubre) and 4 (control) independent set of experiments.

Conditions	Total folates (nmoles per 10^7 parasites)
No drug	10.2 ± 2.6
Rubre 20 μM	3.8 ± 1
Rubre 40 μM	4 ± 2

Table IV. Effect of rubreserine on the GAT activities associated with recombinant *Arabidopsis* GAT-GMPS, AS and GAT-ADCS. Activities were estimated measuring the glutamate production through a GDH coupled assay, as described in Experimental procedures. Rubreserine concentrations up to 50 µM had no detectable effect on GDH activity alone. Assays were made in triplicate and expressed ± SD.

Enzymes	Specific Activities (µmoles min^{-1} mg^{-1})	IC_{50} (µM)
*At*GAT-GMPS	0.30	25 ± 10
*At*AS (α + β subunits)	0.16	7 ± 2
*At*GAT-ADCS	0.40	8 ± 2
GDH (type II from bovine liver)	44	Not measurable: >> 50

Figure 1

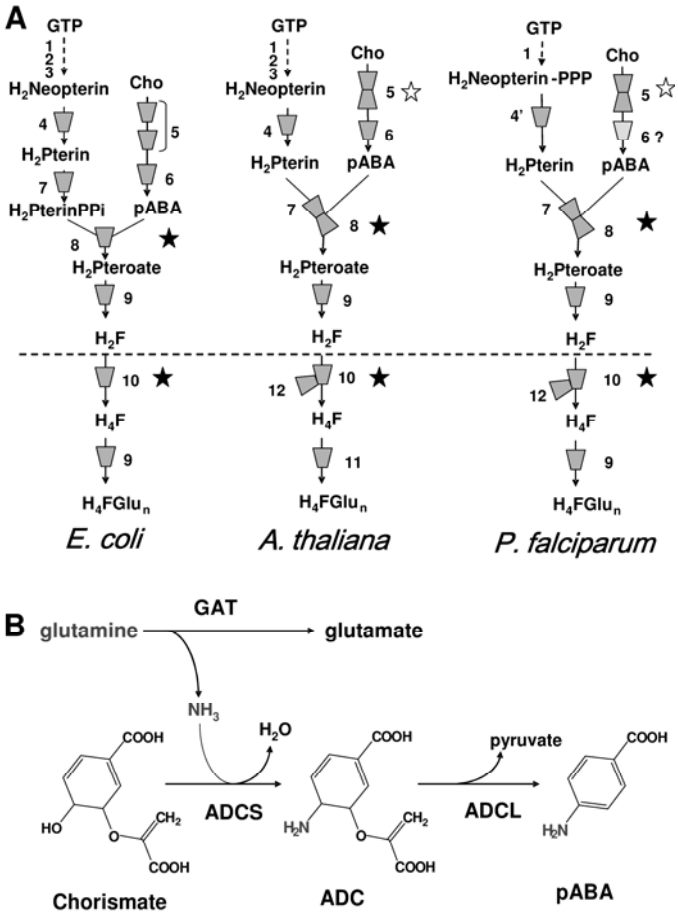
A
GTP
H2Neopterin
Cho
H2Pterin
pABA
H2PterinPPi
H2Pteroate
H2F
H4F
H4FGlun
E. coli
A. thaliana
P. falciparum
H2Neopterin-PPP
B
glutamine
GAT
glutamate
NH3
H2O
ADCS
ADCL
pyruvate
Chorismate
ADC
pABA

Figure 2

Eseroline Rubreserine

Figure 3

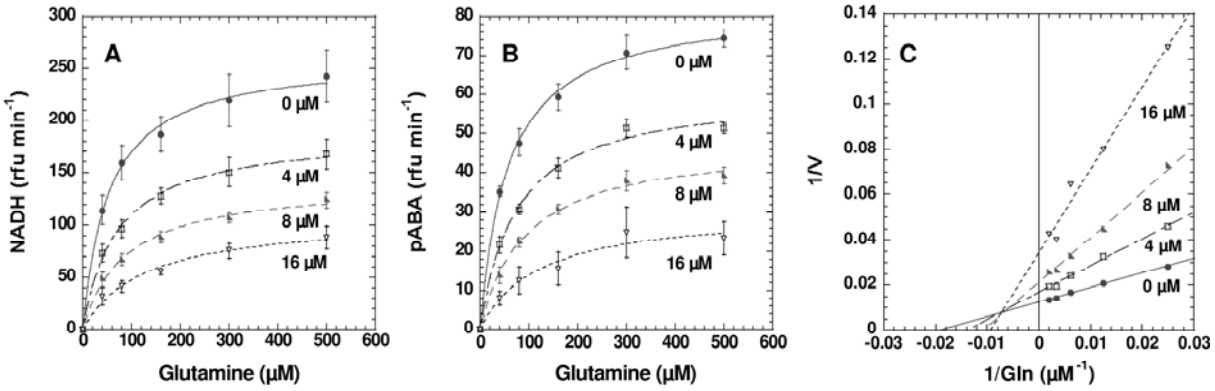
A
NADH (rfu min-1)
Glutamine (μM)
0 μM
4 μM
8 μM
16 μM
B
pABA (rfu min-1)
Glutamine (μM)
0 μM
4 μM
8 μM
16 μM
C
1/V
1/Gln (μM-1)
16 μM
8 μM
4 μM
0 μM

Figure 4

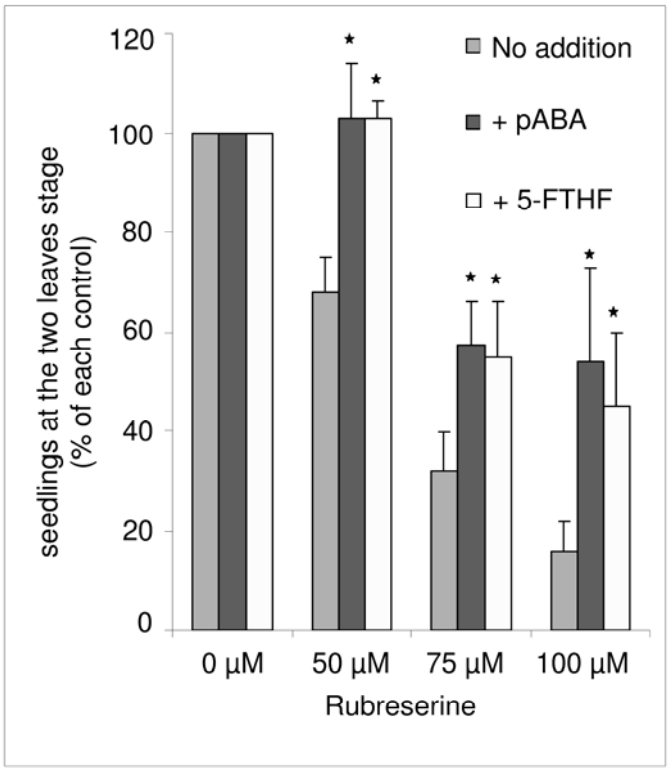
120
100
80
60
40
20
0
seedlings at the two leaves stage
(% of each control)
No addition
+ pABA
+ 5-FTHF
0 µM
50 µM
75 µM
100 µM
Rubreserine

Figure 5

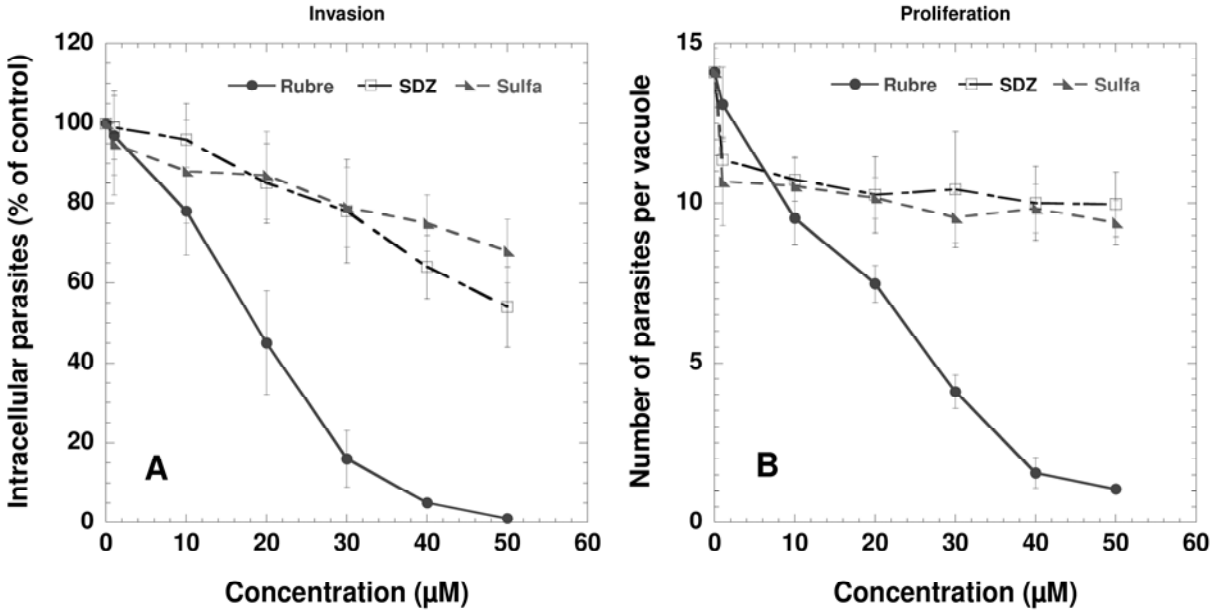
Invasion
Intracellular parasites (% of control)
Rubre
SDZ
Sulfa
A
Concentration (µM)
Proliferation
Number of parasites per vacuole
Rubre
SDZ
Sulfa
B
Concentration (µM)

Figure 6

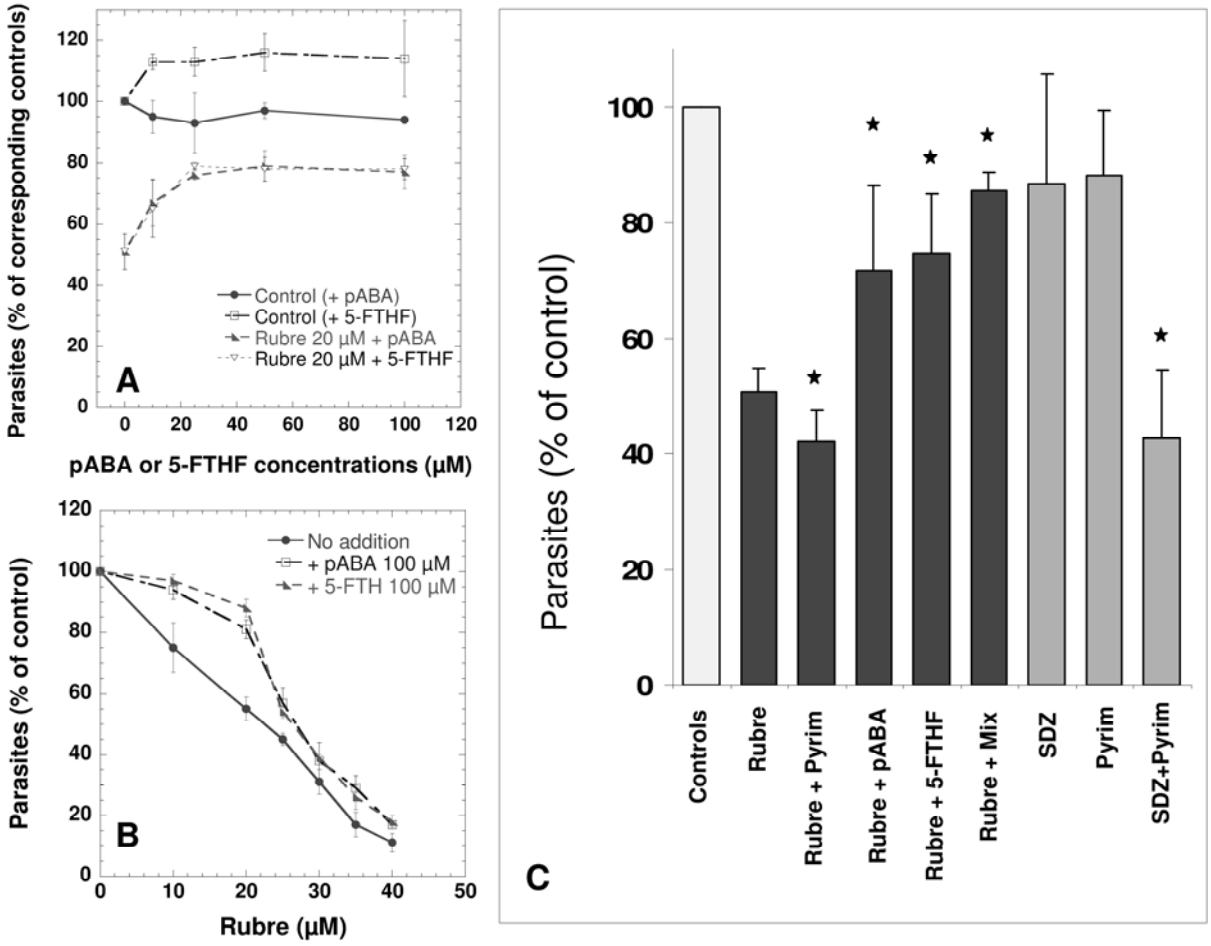
Parasites (% of corresponding controls)
120
100
80
60
40
20
0
0 20 40 60 80 100 120
pABA or 5-FTHF concentrations (µM)
Control (+ pABA)
Control (+ 5-FTHF)
Rubre 20 µM + pABA
Rubre 20 µM + 5-FTHF
A
Parasites (% of control)
120
100
80
60
40
20
0
0 10 20 30 40 50
Rubre (µM)
No addition
+ pABA 100 µM
+ 5-FTH 100 µM
B
Parasites (% of control)
100
80
60
40
20
0
Controls
Rubre
Rubre + Pyrim
Rubre + pABA
Rubre + 5-FTHF
Rubre + Mix
SDZ
Pyrim
SDZ+Pyrim
C

Figure 7

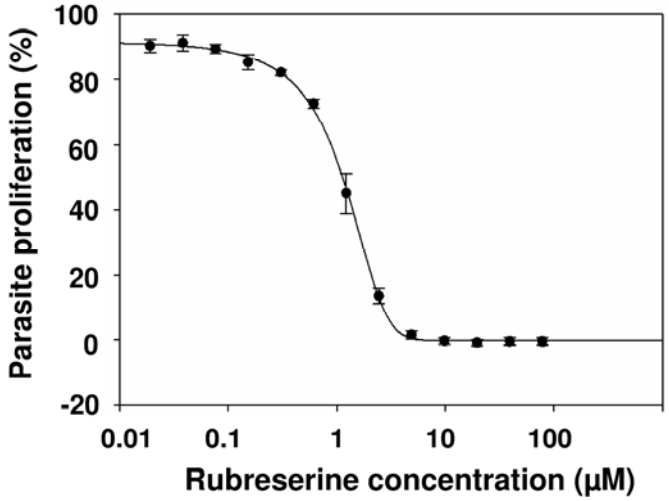
Parasite proliferation (%)
100
80
60
40
20
0
-20
0.01
0.1
1
10
100
Rubreserine concentration (µM)

SUPPLEMENTAL DATA

Supplementary Figure 1: The pH-dependent conversion of eseroline into rubreserine. A) GAT-ADCS inhibition is dependent on the age of the eseroline solution. During this period, the colour of the solution shifted from pinkish to red, suggesting that a product of transformation, rather than eseroline itself, was the inhibitory compound. B) UV-visible spectra of a 500 µM solution of eseroline (24 h old) either in water (pH 3.4 resulting from the presence of fumaric acid in the commercial preparation) or in 50 mM Pi buffer (pH8). Note in the last situation the presence of a peak at 475 nm, characteristic of the red colour of rubreserine. Following the peak at 475 nm, we observed that a 10 mM eseroline solution (pH 8) was converted into rubreserine in about six hours at room temperature (insert). C) ^{13}C-NMR spectra of a 30 mM solution of eseroline (24 h old) showing the appearance at pH 8 of 2 peaks in the carbonyl region of the spectra, characteristic of rubreserine. NMR spectra were recorded on a Bruker NMR spectrometer (AMX 400, WB) equipped with a 10 mm multinuclear probe tuned at 100.6 MHz for ^{13}C NMR studies. The delay D1 between two pulses was set to 60 s to allow a more complete relaxation of carbons in the carbonyl region. D) Reverse phase chromatography of a 24 h old eseroline solution (pH 8) showing one major peak (representing 91% of all peaks detected by their absorbance at 300 nm) with spectra under the peak characteristic of rubreserine. The HPLC conditions were as follow: C_{18} reverse phase column (Zorbax ODS 5µM, 4.6 x 250 mm); flow rate 1 ml min^{-1}; solvent A: 50 mM NaPi, pH 6, 8 mM tetrabutylammonium bisulfate; solvent B: 29 % methanol in solvent A; linear gradient from 17 % to 100 % of solvent B in 15 min, then 100 % B for 9 min; peaks were detected by their absorbance at 300 nm.